

---

**BROADBAND SCATTERING  
OF LASER LIGHT BY  $\beta$ -BaB<sub>2</sub>O<sub>4</sub> CRYSTAL  
PUMPED WITH FEMTOSECOND LASER PULSES**

**O.O. SMYRNOV, D.P. KUDRYAVTZEV, JU.S. OSELEDCHIK,  
A.L. PROSVIRNIN**

PACS 42.65.Lm, 42.65.Dr,  
42.65.Ky  
©2010

Zaporizhzhya State Engineering Academy  
(226, Lenin Av., Zaporizhzhya 69006, Ukraine; e-mail: *asmiralex@yandex.ru*)

---

In the present work, the effect of broadband radiation generation in  $\beta$ -BaB<sub>2</sub>O<sub>4</sub> (BBO) crystals of various orientations pumped with 70-fs pulses of the second harmonic ( $\lambda_{sh} = 390.9$  nm) of a Ti:Sa laser, is investigated. Nonlinear effects, which were observed simultaneously and which lead to the broadband light generation, are interpreted on the basis of experimental data as spontaneous parametric and stimulated Raman scattering of light in the impulsive and highly transient regimes.

broad spectral range ( $\sim 0.195\text{--}2.7$ )  $\mu\text{m}$ , and relatively high radiation resistance [2].

When using BBO crystals, the display of a mixed nonlinearity [2], the direct generation of the third harmonic, and SPS were observed [3, 4]. In work [2], 1- $\mu\text{m}$  picosecond pumping pulses launched the Raman-parametric generation (RPG) of light, and the simultaneous effects of second-harmonic generation and multicomponent RPG in the visible and IR-ranges of the spectrum were observed. In work [5], a BBO crystal was used for the parametric supercontinuum amplification in a single-crystal scheme, while pumping with femtosecond pulses.

In the present work, the results of investigation of the broadband radiation in BBO crystals of three different orientations, pumped with the second harmonic ( $\lambda_{sh} = 390.9$  nm) of a Ti:Sa laser delivering 70-fs pulses with a wavelength of 781.9 nm, are presented. In particular, the work deals with the observation of the effects of SPS under conditions of the vector synchronism and the stimulated Raman scattering. All the crystals were produced in the Laboratory of nonlinear optical converters of the Zaporizhzhya State Engineering Academy.

## 1. Introduction

In recent years, the interest in the investigation of nonlinear optical phenomena observed in the field of femtosecond pulses generated by Ti:Sa and Cr:Forsterite lasers has grown considerably.

The usage of femtosecond lasers allows one to activate not only the quadratic nonlinearity but also high-order nonlinearities, when  $|P_{n+1}/P_n| > 1$ , where  $P_n$  is a polarization of the  $n$ -th order. Thus, it becomes possible to observe nonlinear optical effects related to high-order susceptibilities such as the direct generation of high harmonics, spontaneous parametric scattering (SPS), and stimulated Raman (SRS) and hyper-Raman scatterings.

The investigation of the effectiveness of a transformation of femtosecond pulses in nonlinear crystals requires to consider not only the angle synchronism and the effective nonlinearity, but also the group synchronism of interacting pulses related to their group detuning and the dispersion spreading [1].

A promising material for the investigation of nonlinear effects in the field of ultra-short pulses is the BBO crystal which possesses a high nonlinearity, transparency in the

## 2. Scattering of Laser Light by BBO Crystal

The setup used for studies of the light scattering of the second harmonic of the Ti:Sa femtosecond laser is shown in Fig. 1.

As the source of femtosecond laser pulses with a wavelength of 781.9 nm, a Ti:Sa laser Coherent Mira Optima 900-F with a femtosecond regenerative amplifier Legend

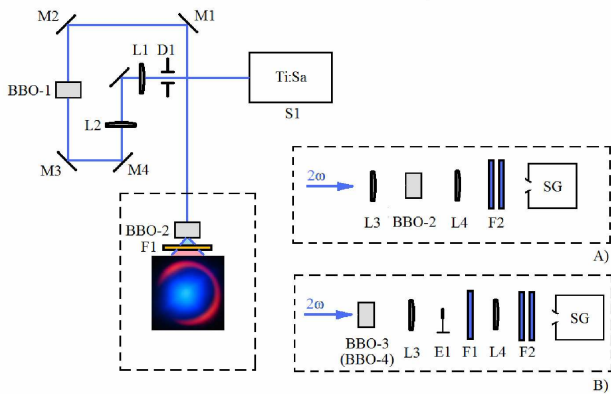


Fig. 1. Experimental setup used in the present work. S1 – source of femtosecond laser pulses; BBO-1 – BBO crystal sample for the second harmonic generation; BBO-2, BBO-3, BBO-4 – BBO crystal samples of different orientations utilized for the investigation of laser light scattering; SG – spectrograph SP-2558 (groove density – 1200 g/mm); L1..L4 – lenses; F1, F2 – filters; E1 – shield; D1 – diaphragm

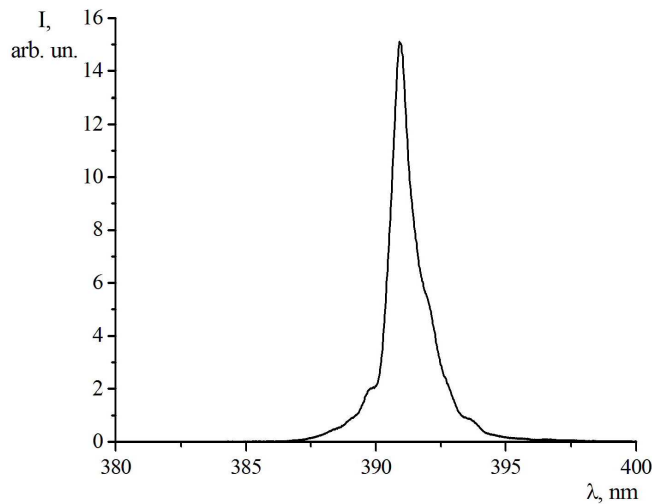


Fig. 2. Spectrum of second harmonic light

F-1K-HE (S1) generating pulses with the 1-kHz repetition rate was used. The utilization of the group velocity external compensator Coherent SPO-1 allowed us to get pulses of 70-fs duration.

The second harmonic was generated in a 3-mm thick crystal BBO-1 oriented for the first type of synchronism, so that the angle to the optical axis constituted 29.2°. The spectrum of the second harmonic is shown in Fig. 2. The FWHM of the spectrum constitutes 1.02 nm (78.6 cm<sup>-1</sup>), and its full bandwidth at the base is ~460 cm<sup>-1</sup>. The power density of a 2ω pumping pulse constituted ~250 GW/cm<sup>2</sup> on the average in all experiments.

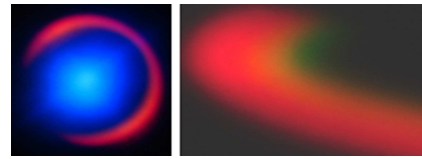


Fig. 3. Radiation at the output of a BBO-2 sample, pumped with the second harmonic of a Ti:Sa laser: a – general view of the output radiation; b – detailed view of the ring zone of the output radiation obtained using a prism

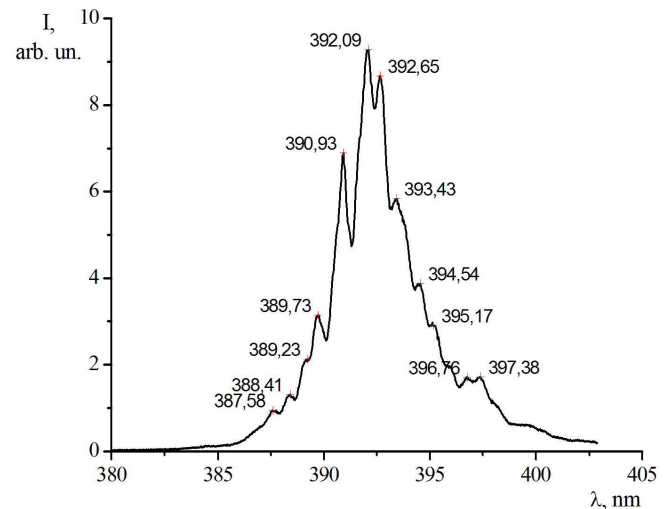


Fig. 4. Spectrum of the central zone of radiation at the output of a BBO-2 crystal sample pumped with the second harmonic of a Ti:Sa femtosecond laser

The investigation of the effect of the second harmonic light scattering by a BBO crystal in the broad spectral region was carried out, using crystals of the following orientations: 1) BBO-2, 3.5 mm long, cut at an angle of 44.3° to the optical axis; 2) BBO-3, 3 mm long, cut at the synchronism angle for the second harmonic generation; 3) BBO-4, 3 mm long, cut in the principal planes. When pumping the BBO-2 crystal with the second harmonic of Ti:Sa laser ( $\lambda_{sh}=390.9$  nm), the intense radiation was generated at the output. The photo of the output radiation with the second harmonic light filtered out by an appropriate filter (F1, Fig. 1, B) is shown in Fig. 3.

As is seen in Fig. 3, two zones of the output radiation can be marked out. The optical setup used for the registration of the spectrum of the central zone is given in Fig. 1, A). The central part of the scattered light was focused on the entrance slit of a spectrograph with lens L4. Neutral light filters F2 at the spectrograph entrance were used for the attenuation of the incident light.

The spectrum of the central zone of the output radiation is shown in Fig. 4.

The spectral broadening of the second harmonic pulse which is observed in Fig. 4 can be attributed to the effect of self-phase modulation (SPM). Because of the fact that the nonlinear coefficient  $n_2$  of the BBO crystal is rather high [6], the SPM process in BBO can take place efficiently. The emergence of a peak structure superimposed on the spectrum broadened by SPM can be attributed to the process of stimulated Raman scattering. According to the theory of SRS [7], three regimes of SRS can be entered depending on the length of a pumping pulse ( $\tau_p$ ), dephasing time of molecular vibrations ( $T_2$ ) and the period of a particular molecular vibrational mode ( $T_v$ ): a) a steady-state regime ( $\tau_p \gg T_2$ ); b) a transient regime ( $\tau_p < T_2$  and the spectral width of a pumping beam  $\Delta\nu_p$  is much broader than the homogeneous broadening of a Raman line  $\Delta\Omega_R = (\pi c T_2)^{-1}$ , so  $\Delta\nu_p \gg \Delta\Omega_R$ ) and c) an impulsive regime ( $\theta_p < T_v$ ). For the BBO crystal,  $T_2 \approx 4.3$  ps [2], and the most intense molecular vibrations derived by us from the spontaneous Raman scattering spectrum occur at  $58 \text{ cm}^{-1}$ ,  $122 \text{ cm}^{-1}$ ,  $159 \text{ cm}^{-1}$ , and  $639 \text{ cm}^{-1}$ . As the pumping pulse duration was  $\sim 70$  fs, and the full bandwidth of pump spectrum at the base constituted  $\sim 460 \text{ cm}^{-1}$ , for the first three Raman vibrations mentioned above, the impulsive regime of SRS (ISRS) was established. In [8], it is noted that ISRS is known to be characterized by a strong deviation of the observed spectral Stokes and anti-Stokes maxima from the Raman lines, which correlates with our observations: the Table presents the predicted and experimentally acquired Stokes and anti-Stokes peak wavelengths corresponding to the  $58\text{-cm}^{-1}$  vibration which is more intense than  $122\text{-cm}^{-1}$  and  $159\text{-cm}^{-1}$  ones.

Since  $\tau_p$  in our experiments was substantially shorter than  $T_2$ , but still longer than  $T_v$  of the most SRS-active mode at  $639 \text{ cm}^{-1}$  [2], the highly transient regime of

**Calculated and experimentally acquired positions of Stokes and anti-Stokes lines, corresponding to  $58\text{-cm}^{-1}$  Raman vibrations**

Stokes peaks		Anti-Stokes peaks	
Theory $\lambda_S$ (nm)	Experiment $\lambda_S$ (nm)	Theory $\lambda_{AS}$ (nm)	Experiment $\lambda_{AS}$ (nm)
391.8	392.1	390.0	389.7
392.7	392.7	389.1	389.2
393.6	393.4	388.3	388.4
394.5	394.5	387.4	387.6
395.4	395.2	386.5	n.p.p*
396.3	396.8	385.7	n.p.p
397.2	397.4	384.8	n.p.p

\* – no pronounced peak.

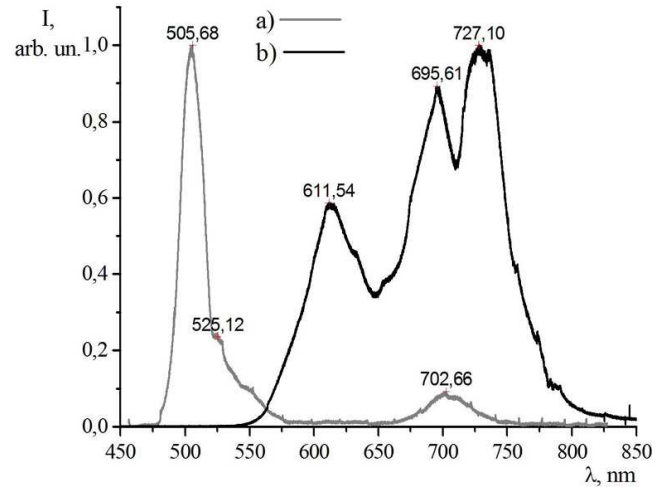


Fig. 5. Spectrum of the ring zone of radiation. a – for BBO-3 crystal sample; b – for BBO-2 crystal sample

SRS was entered for this vibration (HTSRS) [7]. In this regime, competing nonlinear effects can effectively prevent the Raman process from taking place efficiently [7], which explains the absence of the pronounced Stokes line with the  $401\text{-nm}$  wavelength that corresponds to the  $639\text{-cm}^{-1}$  mode.

The spectra of the ring zone of the output SRS radiation observed at BBO-2 and BBO-3 crystal samples are shown in Fig. 5.

For the BBO-4 crystal cut in principal planes, no scattered light was observed. The registration of spectra in Fig. 5 was carried out with the use of an optical setup shown in Fig. 1, B. To block the intense radiation of the central region of the output radiation, shield E1 and filter F1 were introduced into the registration scheme. The radiation of the ring zone was directed into the slit of a spectrograph using lenses L3 and L4.

The following peculiarities of the scattered radiation were noted: 1) the spectrum and the intensity of radiation depend on the rotation of the sample around the normal to its face; 2) the radiation was observed at both sides of the crystal sample; 3) with the denser focusing of the pumping beam by the lens, the enrichment of the spectrum of the output radiation was observed.

Analyzing the experimental results, this effect can be interpreted as the process of parametric interaction under conditions of the non-collinear synchronism.

According to the theory, the effective parametric interaction of three light waves in a quadratic-nonlinear medium requires the fulfilment of two conditions:

$$\omega_1 + \omega_2 = \omega_3, \quad \omega_1 < \omega_2 < \omega_3; \quad k_1 + k_2 = k_3. \quad (1)$$

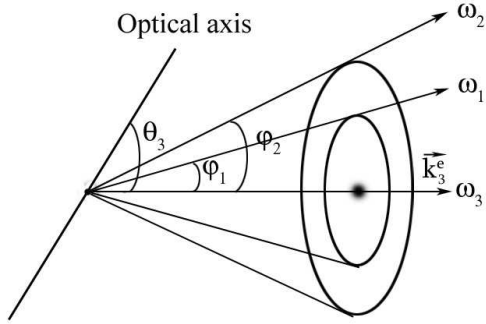


Fig. 6. Scheme of propagation of the pumping  $\omega_3$ , signal  $\omega_1$ , and idler  $\omega_2$  waves under conditions of the non-collinear synchronism

When the pumping wave  $\omega_3$  and reradiated waves  $\omega_1$ ,  $\omega_2$  satisfy the relation  $\omega_3 = \omega_1 + \omega_2$ , the pumping wave amplifies the signal beam  $\omega_2$  in the course of nonlinear coupling simultaneously with the generation of the idler beam  $\omega_1$  according to the condition of phase synchronism:

$$\hbar\mathbf{k}_1 + \hbar\mathbf{k}_2 = \hbar\mathbf{k}_3. \quad (2)$$

Under the conditions of femtosecond pumping for the effective transformation, it is also necessary to fulfil the group velocity matching conditions for the pumping pulse and the pulses of parametric radiation [3].

Relations (1) and (2) can be fulfilled in anisotropic crystals for interacting waves with opposite polarizations. For each type of interaction, the cases of collinear and non-collinear synchronism are possible.

According to the theory, the “*ooe*”, “*oeo*” and “*eo*” synchronism types can be realized in a BBO crystal [9]. We now consider the case of non-collinear “*ooe*” synchronism and assume that an extraordinary wave propagates in the direction forming an angle  $\theta_3$  with the optical axis. Ordinary waves of field fluctuations at frequencies  $\omega_1$  and  $\omega_2$ , amplified as a result of the parametric interaction, will propagate in synchronism directions, unique for each set of parameters  $\gamma$ ,  $\omega_3$ , and  $\theta_3$  and defined by angles  $\phi_1$  and  $\phi_2$  for  $\omega_1$ - and  $\omega_2$ -waves, respectively [9]:

$$\begin{aligned} \phi_1 &= \arccos \left[ \frac{\gamma n_{o1} - (1 - \gamma)n_{o2} + n_{e3}^2(1 - \varepsilon_3^2 \cos^2 \theta_3)^{-1}}{2\gamma n_{o1}n_{e3}(1 - \varepsilon_3^2 \cos^2 \theta_3)^{-1/2}} \right], \\ \phi_2 &= \arccos \left[ \frac{(1 - \gamma)n_{o2} - \gamma n_{o1}}{2(1 - \gamma)n_{o2}n_{e3}(1 - \varepsilon_3^2 \cos^2 \theta)^{-1/2}} + \right. \\ &\quad \left. + \frac{n_{e3}^2(1 - \varepsilon_3^2 \cos^2 \theta_3)^{-1}}{2(1 - \gamma)n_{o2}n_{e3}(1 - \varepsilon_3^2 \cos^2 \theta)^{-1/2}} \right]. \end{aligned} \quad (3)$$

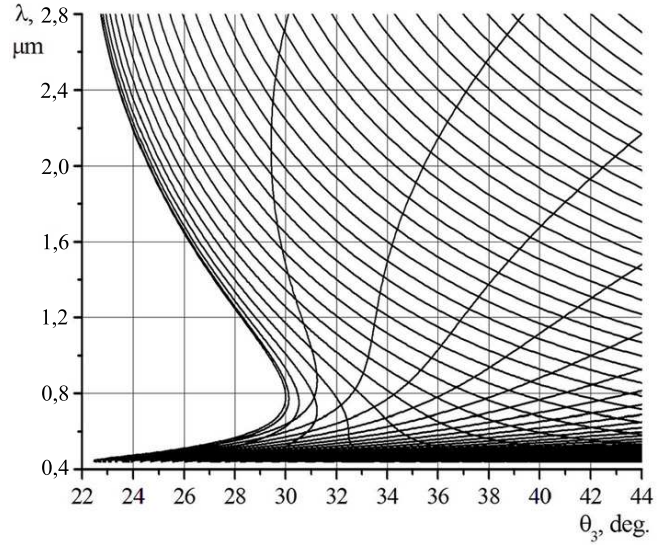


Fig. 7. Family of tuning curves for the OPG process in a BBO crystal

The amplified noise emission (parametric luminescence) at frequencies  $\omega_1$  and  $\omega_2$  propagates along the moving lines of two cones, the cone angles of which are equal to  $\phi_1$  and  $\phi_2$ , respectively, and whose axes coincide with the vector  $\mathbf{k}_3^e$  (Fig. 6).

The relation between the synchronism angle and the parameter  $\gamma$  is described by the tuning characteristics defined by Eqs. (2) and (1). The set of tuning characteristics for a BBO crystal in the range of cone angles  $0 < \phi_1 < 45^\circ$  under the condition of pumping with the second harmonic ( $\lambda_{sh} = 390.9$  nm) is shown in Fig. 7.

As is seen in Fig. 7, in the range of angles  $0^\circ < \theta < 22^\circ$ , the conditions of synchronism cannot be satisfied. This explains the absence of parametric luminescence in BBO-4 crystal sample cut in the principal planes and pumped with the Ti:Sa laser second harmonic radiation along crystal optic axes.

From the obtained tuning characteristics, it also follows that the pumping of BBO-3 crystal sample should result in the parametric luminescence in the ranges of (450–650) nm and (1000–2560) nm. As can be seen from Fig. 5, for BBO-3 crystal sample, radiation in the spectral range of (460–770) nm was observed. This disagreement of wavelengths can be explained by the inaccuracy in the orientation and a slight deflection of the sample position. It is so, because, already at the angle  $\theta_3 = 30^\circ$ , the generation of a parametric spectrum in the range (460–3560) nm becomes possible.

Three pronounced maxima at wavelengths 611.54, 695, and 728 nm in the spectrum of radiation of BBO-2 crystal sample, shown in Fig. 5, can occur as a result of the fulfilled conditions of effective parametric interaction for a number of sets of  $\omega_1$ ,  $\omega_2$ ,  $\omega_3$  frequencies and the conditions of group synchronism for a pumping impulse and signal wave pulses with corresponding wavelengths.

Thus, the observed spectral lines of the ring zone of the observed output radiation correspond to signal waves. Radiation corresponding to idler waves was not registered in the experiment, because the registration equipment sensitivity range constituted (200–1000) nm.

### 3. Conclusions

In this work, the investigation of the broadband light generation at the output of BBO crystal samples of different orientations, pumped with the second harmonic ( $\lambda_{sh} = 390.9$  nm) of a 70-fs Ti:Sa laser, was carried out. In the course of experiments, the peculiarities of the broadband radiation stipulated by the  $\chi_2$  and  $\chi_3$  activities of the BBO crystal are derived. On the basis of the experimental results, it is proposed to consider the observed effect as a result of the simultaneous display of such nonlinear processes as SPM, SRS in impulsive and highly transient regimes and the SPS process in a non-collinear geometry. Special features of ISRS and HTSRS processes, known from the theory tested previously with other materials, agree with those observed in our experiments for BBO. It can be concluded that the BBO crystal possessing a high nonlinear coefficient  $n_2$  and short dephasing times ( $\sim 4.3$  ps) can be effectively used for observations of various nonlinear optic effects in the field of femtosecond pulses.

The work was carried out at the equipment of the Laser Femtosecond Complex of the Institute of Physics of the National Academy of Ukraine (IP NASU). The authors are thankful to the Head of the Department of

Photonic Processes at IP NASU, PhD I.V. Blonsky and to the leading specialist PhD I.M. Dmytruk for their help in organizing and in carrying out the experiments.

1. S.S. Grechin and V.I. Prjalkin, *Quantum Electronics* **8**, 737 (2003).
2. A.A. Kaminski and S.N. Bagaev, *Dokl. Ross. Akad. Nauk* **4**, 468 (1999).
3. V. Krylov and J. Gallus, *Applied Physics* **70**, 163 (2000).
4. A. Nautiyal and B. Prem, *Opt. Commun.* **278**, 175 (2007).
5. P. Wasylczyk and I.A. Walmsley, *Opt. Lett.* **30**, 1704 (2005).
6. R.A. Ganeev, I.A. Kulagin, and A.I. Rysnyanski, *Opt. Commun.* **229**, 403 (2004).
7. E. Sali, P. Kinsler, and G.H.C. New, *Phys. Rev. A* **72**, 013813 (2005).
8. A.S. Grabitchikov, R.V. Chulkov, and V.A. Orlovich, *Opt. Lett.* **28**, 926 (2003).
9. V.G. Dmitriev, and L.V. Tarasov, *Applied Nonlinear Optics*, (Fizmatlit, Moscow, 2004) (in Russian).

Received 13.05.10

#### ШИРОКОСМУГОВЕ РОЗСИЮВАННЯ СВІТЛА В КРИСТАЛІ $\beta$ -BaB<sub>2</sub>O<sub>4</sub> ПРИ НАКАЧЦІ ФЕМТОСЕКУНДНИМИ ЛАЗЕРНИМИ ІМПУЛЬСАМИ

*О.О. Смирнов, Д.П. Кудрявцев, Ю.С. Оселедчик, А.Л. Просвірнін*

#### Резюме

В роботі досліджено явище генерації випромінювання в широкому спектральному діапазоні в кристалах  $\beta$ -BaB<sub>2</sub>O<sub>4</sub> (ВВО) різної орієнтації при накачці фемтосекундними імпульсами другої гармоніки титан-сапфірового лазера із тривалістю імпульсу 70 фс і довжиною хвилі 390,9 нм. На основі експериментальних даних, нелінійні ефекти, які спостерігалися одночасно і привели до широкополосної генерації світла, інтерпретовано як спонтанне параметричне та вимушене комбінаційне розсіювання світла в імпульсному та високо нестационарному режимах.